BIOCHEMISTRY
including biophysical chemistry & molecular biology

ARTICLE

pubs.acs.org/biochemistry

Cardiolipin Deficiency in *Rhodobacter sphaeroides* Alters the Lipid Profile of Membranes and of Crystallized Cytochrome Oxidase, but Structure and Function Are Maintained

Xi Zhang,[†,‡] Banita Tamot,[†] Carrie Hiser,[†] Gavin E. Reid,[†,‡] Christoph Benning,[†] and Shelagh Ferguson-Miller*[,†]

[†]Department of Biochemistry and Molecular Biology and [‡]Department of Chemistry, Michigan State University, East Lansing, Michigan 48824, United States

Supporting Information

ABSTRACT: Many recent studies highlight the importance of lipids in membrane proteins, including in the formation of well-ordered crystals. To examine the effect of changes in one lipid, cardiolipin, on the lipid profile and the production, function, and crystallization of an intrinsic membrane protein, cytochrome *c* oxidase, we mutated the cardiolipin synthase (*cls*) gene of *Rhodobacter sphaeroides*, causing a >90% reduction in cardiolipin content in vivo and selective changes in the abundances of other lipids. Under these conditions, a fully native cytochrome *c* oxidase (C*c*O) was produced, as indicated by its activity, spectral properties, and crystal characteristics. Analysis by MALDI tandem mass spectrometry (MS/MS) revealed that the cardiolipin level in C*c*O crystals, as in the membranes, was greatly decreased. Lipid species present in the crystals were directly analyzed for the first time using MS/MS, documenting their identities and fatty acid chain composition. The fatty acid content of cardiolipin in *R. sphaeroides* C*c*O (predominantly 18:1) differs from that in mammalian C*c*O (18:2). In contrast to the cardiolipin dependence of mammalian C*c*O activity, major depletion of cardiolipin in *R. sphaeroides* did not impact any aspect of C*c*O structure or behavior, suggesting a greater tolerance of interchange of cardiolipin with other lipids in this bacterial system.

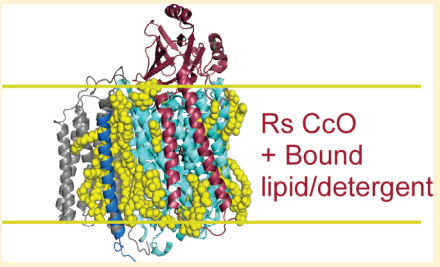

Lipids are resolved in the crystal structures of many membrane proteins, implying a significant role in protein structure and function.[1,2] Specific lipids have been shown to be required for correct folding and assembly of several membrane proteins, including the plant light-harvesting complex[3] and the bacterial lactose permease.[4−6] Other studies of bovine and yeast cytochrome bc_1, bovine cytochrome *c* oxidase, and bacterial KcsA K^+ channel indicate a requirement for specific lipids for full activity.[7−12] In some cases, complete removal of bound lipid in vitro results in abolishment of protein function, an effect that is reversed by adding back certain types of lipids.[11−13] Investigating the roles of bound lipids is therefore an important part of understanding the mechanism and regulation of membrane proteins.

Lipids are found to stabilize membrane protein structure,[14] and therefore, retention of lipid molecules during purification has been emphasized as an important factor in the successful crystallization of membrane proteins.[2,15] The observation that the quality of *Escherichia coli* lactose permease crystals can be controlled by changing the phospholipid content[16] demonstrates this principle. Similarly, the crystallization of the cytochrome b_6f complex was improved by the addition of lipids.[14] Efforts to obtain high-resolution structures of membrane proteins thus demand closer scrutiny of the role of protein-associated lipid molecules.

The terminal enzyme of the respiratory electron transport chain, cytochrome *c* oxidase (C*c*O),[17,18] has served as a model system for studying the involvement of lipids in membrane protein structure and function[19,20] because its spectrally accessible metal centers provide sensitive intrinsic probes for monitoring structural integrity and activity. A number of lipid molecules copurify with C*c*O from bovine heart and *Rhodobacter sphaeroides*, and the lipid binding sites identified crystallographically in the core subunits of C*c*O are highly conserved from bacteria to mammals,[2,21,22] suggesting an important role not only in function but also in achieving high-resolution crystal structures of C*c*O.

Cardiolipin (CL) is one lipid whose requirement has been established by biochemical studies of a number of membrane proteins, particularly respiratory chain complexes from both bacterial and mitochondrial sources.[7,10,11,23,24] Its unique structure, composed of two phosphates, three glycerols, and four hydrophobic fatty acid chains, allows cardiolipin to bind to membrane proteins more tenaciously than lipids with only two alkyl chains. Recent evidence suggests that it can act as a glue between proteins that form supercomplexes in membranes[25,26] and that it plays a role in the signaling system that controls apoptosis in eukaryotic cells.[27,28] It has also been reported to be essential for the full activity of mammalian heart C*c*O,[7,29] but most of these studies removed CL

Received: October 21, 2010
Revised: April 7, 2011
Published: April 08, 2011

in vitro after the enzyme was purified. In contrast, several in vivo studies in yeast report that a deficiency in cardiolipin did not significantly affect the activity of C*c*O, nor did it alone cause mitochondrial dysfunction.[30−32] However, the deficiency of both phosphatidylglycerol (PG) and CL resulted in very little C*c*O production and severely dysfunctional mitochondria,[30] suggesting CL can be functionally replaced by PG but not other lipids in yeast.

To test if CL is strictly required in C*c*O from the purple nonsulfur bacterium *R. sphaeroides*, C*c*O was expressed in a CL-deficient mutant created by deleting the *cls* gene encoding CL synthase. The expression, activity, structure, crystallization, and lipid composition of C*c*O were examined. The results support a flexible lipid requirement in this bacterial enzyme.

MATERIALS AND METHODS

Media and Growth Conditions. All *R. sphaeroides* strains were grown in Sistrom's succinate-basal salts medium.[33,34] The cells were grown on agar-solidified medium or in liquid cultures at 30 °C under anaerobic photoheterotrophic[35] or aerobic chemoheterotrophic[36] conditions, as previously described. When required, ampicillin (50 μg/mL), kanamycin (25 μg/mL), tetracycline (1 μg/mL), chloramphenicol (25 μg/mL), streptomycin (5 μg/mL), or spectinomycin (5 μg/mL) was added to the media. *E. coli* cells were grown in LB medium at 37 °C, and when required, antibiotics were added to the solid medium or liquid cultures at a concentration of ampicillin, kanamycin, or chloramphenicol of 50 μg/mL.

For photosynthetic growth curves, strains 2.4.1 (wild-type, CL+)[37] and CL3 (*cls* deletion, CL−) were grown in 250 mL sidearm flasks filled completely with Sistrom's medium under approximately 30 μmol m^{-2} s^{-1} light without shaking. For aerobic growth curves, strains 2.4.1 and CL3 were grown at 30 °C in 50 mL of Sistrom's medium in 250 mL sidearm flasks with vigorous shaking (250 rpm). In each case, cell densities were measured in a Klett photometer with a #66 filter. Note that 1 Klett unit is equivalent to 10^7 cells/mL.[38]

Construction of Plasmid pSUP-CLD. Using genomic DNA from wild-type strain 2.4.1 as a template, a 600-nucleotide region of the *cls* gene (GenBank entry YP_353546 coding sequence, nucleotides 1−600) was amplified via polymerase chain reaction (PCR) using primers P1 (5′-GCGGGATCCATGATCGACGACTGGCTGGGCGTCC-3′) and P3 (5′-GCGGTCGACGTTGCGCCCGCCCACGATGGCC-3′, *Sal*I). Similarly, a 591-nucleotide region of the gene (GenBank entry YP_353546 coding sequence, nucleotides 961−1551) was amplified by using another set of primers, P2 (5′-GCGAAGCTTGGATCCTCAGAGGTAGCTCTGGATCG-3′, *Hin*dIII, *Bam*HI) and P4 (5′-GCGGTCGACGGCGAGGCGATCACCGCGCTCC-3′, *Sal*I). The amplified products were cloned into vectors pPICT-2 and pGEM-T Easy (Promega, Madison, WI) to generate plasmids pPICT-2-I and pGEM-T-II, respectively. Segment II from plasmid pGEM-T-II was cut out by double digestion with *Sal*I and *Hin*dIII and was ligated into pPICT-2-I, which had been digested with the same enzymes to generate plasmid pPICT-2-I/II. From the pUC4K plasmid (GE Healthcare, Piscataway, NJ), the kanamycin resistance cassette (*kan*R) was cut out by using *Sal*I sites placed on either side of the gene and was subsequently inserted into plasmid pPICT-2-I/II, which had been digested by the same enzymes. The resulting pPICT-2-CK plasmid contained the *kan*R cassette inserted between segments I and II. The orientation of *kan*R was checked by digesting plasmid pPICT-2-CK with *Hin*dIII. Because a *Hin*dIII site is placed asymmetrically within *kan*R, digestion by the enzyme would produce fragments of different sizes based upon the orientation of the gene.[39] Using *Bam*HI, the entire gene construct was cut out from plasmid pPICT2-CK and was ligated into suicide plasmid pSUP202[40] by using the *Bam*HI site placed within the tetracycline resistance gene, yielding plasmid pSUP-CLD.

Disruption of the *cls* Gene in *R. sphaeroides* 2.4.1. Plasmid pSUP-CLD was mobilized into wild-type strain 2.4.1[39] by using *E. coli* strain S17-1 (RP4−2-Tc::Mu-Km::Tn7Tp^{r}Sm^{r}Pro$^-$)[40] as a donor. Through selection for kanamycin (100 μg/mL) resistance, the plasmid was forced to recombine with the genome using the regions homologous to the *cls* gene. The exconjugants with double crossovers were selected by ampicillin and chloramphenicol sensitivity.[39] The resulting mutant strain of *R. sphaeroides* was called CL3. The gene disruption in the mutant was verified by PCR.

Quantitative Membrane Lipid Analysis Using Thin-Layer Chromatography and Radioactive Labeling. Cultures of wild-type and mutant strains were grown aerobically overnight. Lipids were then labeled via incubation of the cultures with [1-^{14}C]-acetate as described previously.[41] Cells were collected by centrifugation and washed twice and suspended in 50 μL of water. From the cells, lipid extracts were prepared and loaded onto activated silica thin-layer chromatography (TLC) plates (Si250; Baker) as previously described.[35] The lipids were separated by two-dimensional TLC using a chloroform/methanol/water mixture (65:25:4, v/v/v) for the first dimension and a chloroform/methanol/acetic acid/water mixture (170:25:25:4, v/v/v/v) for the second dimension. Lipids were visualized by being charred with 50% H_2SO_4.[42]The plates were then exposed to a phosphoimager (GE Healthcare) to obtain an image of the labeled lipids. The lipids on the TLC plates were then visualized by iodine staining, and the radioactivity in the individual spots was measured by using a liquid scintillation counter.[41] The relative amount of each lipid was calculated as the percentage of total radioactivity present in the lipid sample.

Engineering *R. sphaeroides* 2.4.1 and CL3 Strains To Overproduce C*c*O. To overproduce a histidine-tagged version of the C*c*O enzyme, the pRK-pYJ123H plasmid[36] carrying the genes encoding a wild-type C*c*O was transferred by conjugation from *E. coli* S17-1 into *R. sphaeroides* strains 2.4.1 and CL3 as described previously[36] to create strains 2.4.1+C*c*O (CL+) and CL3+C*c*O (CL−), respectively. These strains were grown aerobically in Sistrom's medium containing 1 μg/mL tetracycline.

To overproduce a version of C*c*O suitable for crystallization, a histidine tag on subunit II and a shortened version of subunit IV are required to improve molecular homogeneity.[2] Therefore, the pCH169 plasmid[2] carrying these versions of the C*c*O genes was transferred by conjugation into the CL3 mutant strain to create strain 169/CL3 (Table S1 of the Supporting Information). The CL(+) crystallography strain used as the control herein is 169, which is derived from a 2.4.1 C*c*O deletion strain (YZ200[36]) and carries the pCH169 plasmid.[2]

The lipid compositions of the membranes from the two different strains without the *cls* deletion [2.4.1+C*c*O and 169, both termed WT or CL(+)] were found to be the same, by mass spectrometry lipid analysis. Similarly, the two strains carrying the *cls* deletion [CL3+C*c*O and 169/CL3, both termed CL(−)] also exhibited the same lipid profile (data not shown), as expected because these strains are derived from the same parent strain,

CL3.[43] All strains used for C*c*O production in this study are listed in Table S1 of the Supporting Information.

C*c*O Purification, Characterization, and Crystallization. *R. sphaeroides* strains overexpressing six-histidine-tagged C*c*O were grown aerobically in Sistrom's medium with appropriate antibiotics as described previously.[36] C*c*O protein was purified by using nickel affinity chromatography and monitored by UV−vis spectroscopy (dithionite-reduced minus ferricyanide-oxidized or dithionite-reduced only).[36] C*c*O protein for crystallization was purified as described previously.[2] Maximal rates of consumption of oxygen by purified C*c*O were measured polarographically in 50 mM KH_2PO_4 (pH 6.5) with 0.05% (m/v) lauryl maltoside, 1 mM *N*,*N*,*N*′,*N*′-tetramethyl-*p*-phenylenediamine (TMPD), 2.8 mM ascorbate, and 30 μM cytochrome *c* as the substrate and in the absence or presence of externally added lipids [a mixture of soybean asolectin at a final concentration of 0.44 mg/mL (Avanti Polar Lipids, Alabaster, AL) and cholate at a final concentration of 0.02%]. The enzymatic activity (turnover number; moles of cytochrome *c* oxidized per mole of enzyme per second) was calculated as described previously.[44] Total protein amounts were determined by using the bicinchoninic acid protein assay kit (Pierce, Rockford, IL), including 0.25% deoxycholate in the buffer.[45] Four-subunit and two-subunit C*c*O protein crystals were obtained using methods described previously[46] for the crystallization-optimized strains.

Direct Mass Spectrometry Analysis of Lipids in Membranes and Protein Crystals. Mass spectrometry (MS) and tandem mass spectrometry (MS/MS) analyses of lipids in the isolated membranes and C*c*O protein crystals were performed using a linear quadrupole ion trap mass spectrometer equipped with a vacuum matrix-assisted laser desorption ionization ion source (model vMALDI-LTQ, Thermo Scientific, San Jose, CA). Protein crystals were rinsed briefly in water at 4 °C to remove residual protein precipitate and other well solution components loosely attached to the surface of the crystals before they were redissolved by being extensively vortexed in water. One microliter of either resuspended membrane (at a protein concentration of 0.25 mg/mL determined by the BCA assay using bovine serum albumin as the standard) or 1 μL of a redissolved C*c*O crystal solution (at a C*c*O concentration of 8.3 μM, equivalent to 1.00 mg of protein/mL, determined by the BCA assay using a purified C*c*O solution with a known concentration as the standard) was applied to individual spots on the stainless steel sample plate and dried in air. Subsequently, 1 μL of 0.1 M (for membrane samples) or 0.5 M (for crystal samples) 2,5-hydroxybenzoic acid (2,5-DHB) (Sigma-Aldrich, Milwaukee, WI) was added; acetonitrile (Mallinckrodt Chemicals, Philipsburg, NJ) and water (2:1, v/v). MS and MS/MS spectra were acquired in negative and positive ion modes using enhanced resonance ejection scan conditions. MS/MS spectra were recorded using collision-induced dissociation (CID) typically at a normalized collision energy of 30%, an isolation width of 1.0 or 1.2, and an activation Q value of 0.2. The spectra shown are the average of 250 scans.

RESULTS

Identification of a Gene Encoding CL Synthase in *R. sphaeroides*. Because the gene encoding CL synthase (*cls*) had not been previously identified in *R. sphaeroides*, the candidate *cls* gene of *R. sphaeroides* (GenBank entry YP_353546) was selected on the basis of similarity to the amino acid sequence of *E. coli* CL synthase (27% identical and 44% similar using BLAST[47]). The candidate gene was cloned into *E. coli* expression plasmid pQE-30 (Qiagen, Valencia, CA) and transformed into *E. coli* CL-deficient strain SD9.[48] Thin-layer chromatograms of extracts from the SD9 transformant harboring the *cls* expression plasmid showed the presence of CL, while no CL was observed for SD9 transformed with the empty vector.[43] These results suggest that the *R. sphaeroides cls* gene functionally complements the *E. coli* CL-deficient mutant and thus encodes a CL synthase of *R. sphaeroides*.

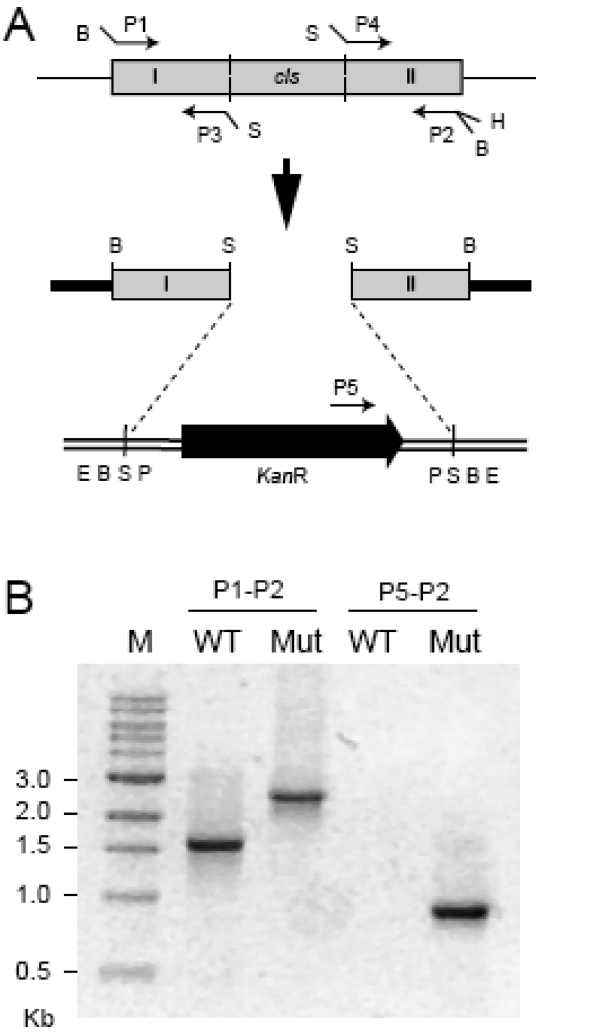

Figure 1. Disruption of the *cls* gene. (A) Schematic diagram showing the gene disruption strategy. Gray boxes represent the *cls* gene and amplified segments of the gene. The black block arrow represents the kanamycin resistance cassette, and the direction of the arrowhead shows its orientation. Plasmids pPICT-2 and pUC4K are shown as thick solid lines and double lines, respectively. Restriction sites: B, *Bam*HI; S, *Sal*I; H, *Hin*dIII; E, *Eco*RI; P, *Pst*I. (B) PCR verification of gene disruption. Genomic DNA was isolated from the wild-type (WT) and *cls*-deleted mutant (Mut) strains, and two polymerase chain reactions were conducted using different sets of primers placed at the positions indicated in Figure 2A. The sizes of the PCR products were compared by gel electrophoresis. M indicates the marker lane.

Construction of the *R. sphaeroides* CL Synthase Mutant. The genomic copy of the *cls* gene was replaced by a disrupted copy carried by plasmid pSUP-CLD, yielding a CL synthase-deficient mutant of *R. sphaeroides* (Figure 1A). Gene disruption

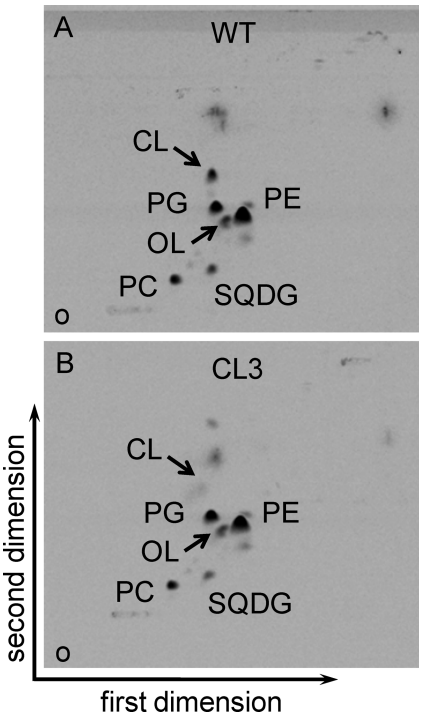

Figure 2. Two-dimensional thin-layer chromatogram of ^{14}C-labeled lipids from aerobically grown *R. sphaeroides* (A) wild-type strain 2.4.1 and (B) the *cls*-deleted mutant CL3. The lipids were visualized by using a phosphoimager. Abbreviations: PE, phosphatidylethanolamine; PG, phosphatidylglycerol; PC, phosphatidylcholine; SQDG, sulfolipid; OL, ornithine lipid; CL, cardiolipin; O, origin.

was confirmed by PCR analysis of genomic DNA. The PCR amplification using the primers specific for the two ends of the *cls* gene (P1 and P2) gave a larger amplified product in the mutant than in the wild type (Figure 1B). The size of the amplified product in the mutant (approximately 2.6 kb) equaled the sum of the sizes of the kanamycin resistant cassette (1.2 kb) plus the 5′ region (0.6 kb) and 3′ region (0.59 kb) of the *cls* gene that had been amplified and used for obtaining the gene disruption construct. A second PCR using *cls* gene specific primer P2 and kanamycin resistant gene specific primer P5 gave a product of the expected size (approximately 0.96 kb) in the mutant, whereas no amplification was seen in the wild type (Figure 1B). TLC analysis of the lipid extracts from the wild type and the mutant (designated CL3) showed a strong reduction in the level of CL in the mutant (Figure 2). The result clearly indicated that the inactivation of the *cls* gene impaired CL synthesis in the mutant.

Composition of General Lipid Types in Wild-Type and Mutant Cells. To determine the effect of *cls* gene inactivation on lipid content, we used a saturation [^{14}C]acetate labeling approach to obtain a quantitative comparison of relative lipid amounts in the wild type and the CL3 mutant. The level of CL in the mutant was strongly reduced, but a trace of CL, <10% of that in the wild type, was still present in the mutant (Table 1). The result was consistent with that observed for an *E. coli cls* knockout mutant, in which a low level of CL was also still present.[49] Corresponding to the decrease in CL in the CL3 mutant, an increase in the level of PG, the precursor for CL synthesis, was observed (Table 1). Within statistical limitations, the amounts of phosphatidylcholine (PC), phosphatidylethanolamine (PE), ornithine lipid (OL), and sulfoquinovosyldiacylglycerol (SQDG) remained relatively unchanged. The structures of the molecular species in each type of lipid in the cell membranes were elucidated by MALDI MS and MS/MS as well as ESI MS, MS/MS, and multistage tandem mass spectrometry (MS^n) in the linear ion trap mass spectrometer.[50] The changes in the amounts of phospholipids revealed by TLC were confirmed by quantitative ESI analysis of the phospholipids using internal standards in both MS and MS/MS [see the companion paper (DOI 10.1021/bi1017039)].

Table 1. Lipid Composition of the *R. sphaeroides* Wild Type (2.4.1) and CL-Deficient Mutant (CL3) Determined by Thin-Layer Chromatograpy and Radioactive Labeling[a]

lipid	wild type	CL3
CL	5.6 ± 1.6	0.5 ± 0.1
OL	3.7 ± 0.2	3.5 ± 0.4
PE	42.4 ± 4.3	44.1 ± 2.5
PG	22.4 ± 0.1	26.2 ± 2.2
SQDG	6.7 ± 0.2	6.4 ± 1.3
PC	19.2 ± 4.4	19.2 ± 3.8

[a] The values represent the mean percentage of radioactivity for individual lipids ± the standard error from three independent experiments. Abbreviations: CL, cardiolipin; PE, phosphatidylethanolamine; OL, ornithine lipid; PG, phosphatidylglycerol; SQDG, sulfoquinovosyldiacylglycerol; PC, phosphatidylcholine.

Effect of CL Deficiency on *R. sphaeroides* Cell Growth. To analyze the effect of the decreased level of CL on the overall growth of *R. sphaeroides* cells, the photosynthetic and respiratory growth of the wild type and the mutant was compared. Under the conditions used in this study, no significant differences were observed in the photosynthetic growth of either line (Figure 3A). Respiratory growth was slightly reduced in the mutant, as indicated by the increased lag time (slower approach to final cell density) and lower final cell density (Figure 3B). The results suggest that CL may contribute to optimal respiratory growth but may be less critical to photosynthetic growth.

Production of C*c*O in *R. sphaeroides* Wild-Type and CL-Deficient Cells. The wild-type 2.4.1 strain of *R. sphaeroides* naturally produces a low level of C*c*O in its membranes when grown under aerobic conditions (Figure 4A). Because this strain has previously been used to produce a variety of lipid mutants,[39,42,51] it was necessary to demonstrate that it is also a suitable host for C*c*O overproduction to provide the model system for testing the role of lipids in this protein. Optical difference spectra of reduced minus oxidized states provide a facile method for assessing the level of C*c*O in the membrane by the absorbance of its *a*-type hemes. Difference spectra of the solubilized membrane proteins of the wild-type 2.4.1 strain (Figure 4A) showed that the 606 nm peak, representing *a*-type hemes of C*c*O, was much smaller than the 560 nm peak to which the spectra are normalized. (Note that the 560 nm peak represents *b*-type hemes of the bc_1 complex plus a cbb_3 oxidase also present in the membranes. In addition, a membrane-bound cytochrome *c* contributes to the 550 nm region.) After the C*c*O genes were introduced on plasmid pRK-pYJ123H to create strain 2.4.1+C*c*O, the intensity of the 606 nm peak was strongly increased relative to that of the 560 nm peak, indicating an overproduction of C*c*O (Figure 4B). This was confirmed by measuring the concentration of C*c*O per milligram of total protein, which showed an equivalent increase. When this plasmid was introduced into CL-deficient strain CL3, high levels of C*c*O

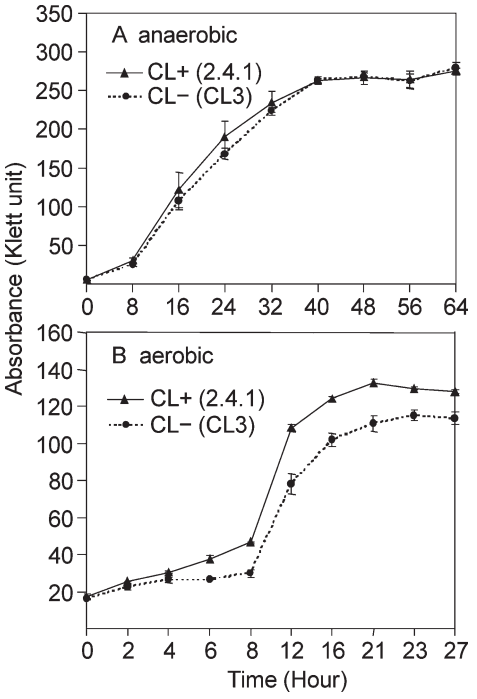

Figure 3. Growth curves of *R. sphaeroides* wild-type (▲; 2.4.1) and CL-deficient mutant (●; CL3) strains under (A) anaerobic photoheterotrophic growth and (B) aerobic chemoheterotrophic growth conditions, both in Sistrom's medium at 30 °C. The data are the average of three independent growth cultures, and the error bars are the standard deviations. Absorbances are expressed in Klett units, where 1 Klett unit is equivalent to 10^7 cells/mL.[38]

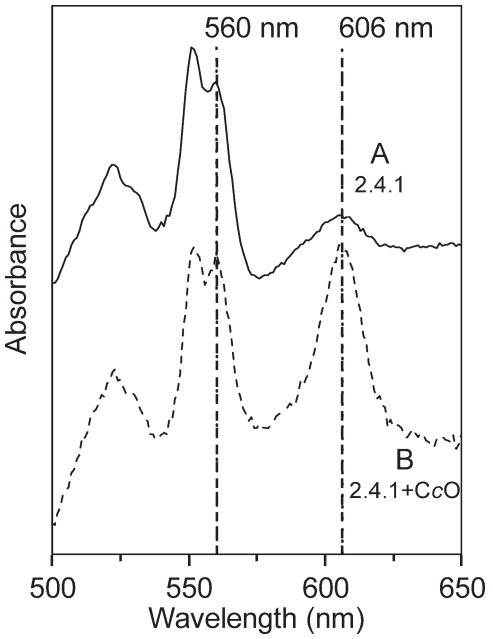

Figure 4. Optical difference spectra of dithionite-reduced minus ferricyanide-oxidized solubilized membranes from *R. sphaeroides* strains (A) 2.4.1 (wild type) and (B) 2.4.1+C*c*O (wild type with C*c*O genes added on expression plasmid PRK- pYJ123H). The relative levels of C*c*O are indicated by the sizes of the *a*-type heme absorbance peaks at 606 nm compared to the sizes of the *b*-heme peaks at 560 nm. The spectra are normalized to the 560 nm (*b*-type heme) peak. (Note that these membranes also contain the bc_1 complex, a cbb_3-type oxidase, and a membrane-bound cytochrome *c* that all contribute to the 560 and 550 nm peaks.)

expression were also seen but were variable depending on the culturing time and volume of the culture (data not shown). In lower-volume cultures, the levels of C*c*O were high, while they were sometimes lower in larger cultures grown for longer times. This observation indicates a possibly greater sensitivity of the CL3 mutant to the stress experienced during subculturing and dilution into larger flasks [see also the companion paper (DOI 10.1021/bi1017039)].

Properties of C*c*O Purified from Wild-Type and *cls* Mutant Cell Lines. Table 2 lists the spectral properties and enzymatic activities of C*c*O protein purified from *R. sphaeroides* cell lines overproducing a histidine-tagged version of C*c*O. The Soret (445 nm) and α (606 nm) bands in the optical spectra are diagnostic of the native, reduced heme centers of C*c*O. No wavelength shifts of peak maxima were observed between the CL(−) mutant cell line (CL3+C*c*O) and the CL(+) control (2.4.1+C*c*O), indicating that the absence of the *cls* gene in the mutant did not impair its ability to correctly assemble and insert the metal centers into C*c*O. The enzymatic activities of C*c*O purified from strains CL(−) and CL(+) were also very similar, indicating that the enzyme purified from the CL(−) mutant cells was as active as that purified from the CL(+) cells. The activities of all purified C*c*Os increased similarly in the presence of externally added lipids during the assay. This commonly observed phenomenon is likely related to the extent of delipidation of C*c*O during the purification process.[44] When tested for stability at temperatures ranging from 20 to 80 °C, C*c*O purified from both the wild-type and mutant strains behaved similarly (data not shown).

SDS−PAGE analysis of C*c*O purified from CL(+) and CL(−) mutant strains indicated that the composition and relative levels of all of the subunits were similar [see the companion paper (DOI 10.1021/bi1017039)].

MALDI MS Analysis of Lipids in the Membranes Overexpressing C*c*O. Panels A and B of Figure 5 show the negative ion mode MALDI MS spectra of the lipids in the isolated membranes of the CL(+) and CL(−) strains of *R. sphaeroides*. Similar types of lipids were observed in the membranes of both strains, including PE, PG, SQDG, and CL, although their abundances varied. The major molecular species of lipids detected in these strains include phospholipids PE 18:1/18:1 (*m*/*z* 742.5) and PG 18:1/18:1 (*m*/*z* 773.5); cardiolipins $CL(18:1)_4$ (*m*/*z* 1456.0), $CL(16:1)_1(18:1)_3$ (*m*/*z* 1428.0), $CL(16:0)_1(18:1)_3$ (*m*/*z* 1430.0), and $CL(18:0)_1(18:1)_3$ (*m*/*z* 1458.0); and sulfolipids SQDG 16:0/16:0 (*m*/*z* 793.5), SQDG 16:0/18:1 (*m*/*z* 819.5), SQDG 16:0/18:0 (*m*/*z* 821.5), SQDG 18:1/18:1 (*m*/*z* 845.5), and SQDG 18:0/18:1 (*m*/*z* 847.5). The identities of each of the membrane lipid species labeled in these figures were confirmed by MS/MS analysis.[50] Note that although MALDI is not generally considered to be a rigorously quantitative method because of issues arising from matrix and sample heterogeneity, these experiments were performed in parallel under identical sample handling and data acquisition conditions and in multiple replicates, giving confidence in a semiquantitative interpretation of the data, particularly using MS/MS, because the chemical noise observed during MS analysis is mostly eliminated.[52] Further, MALDI has the major advantage of being able to analyze samples directly, without chemical solvent extraction, and being more tolerant of the presence of detergent than ESI, thus bypassing problems caused by detergents and detergent removal

Table 2. Spectral and Enzymatic Properties of CcO Purified from *R. sphaeroides* Wild-Type (2.4.1+CcO) and Cardiolipin-Depleted (CL3+CcO) Cell Lines[a]

		spectral peaks of purified CcO (nm)				
cell line	genotype	Soret	α	activity (s^{-1}) with no added lipid	activity (s^{-1}) with added lipid	increase in activity with lipid (%)
2.4.1+CcO	wild type	445	606	1050 ± 100	1340 ± 50	28 ± 2
CL3+CcO	Δ*cls*	445	606	1060 ± 109	1410 ± 120	33 ± 8

[a] Both strains produced His-tagged CcO from a plasmid (PRK-pYJ123H[36]). The Soret and α peaks were from the optical spectra of dithionite-reduced CcO. The molecular activity of purified CcO was measured at pH 6.5 and presented as turnover number (moles of cytochrome *c* oxidized per mole of CcO per second). The number of independent measurements was three for 2.4.1+CcO and five for CL3+CcO.

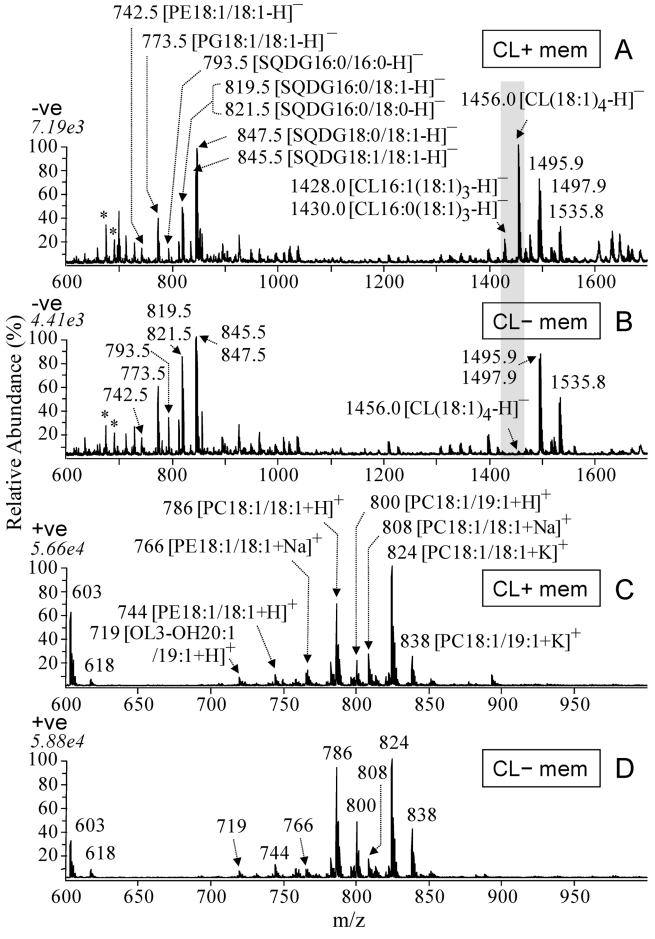

Figure 5. MALDI-MS spectra of membranes isolated from CL(+) (169WT) and CL(−) (169CL3) strains of *R. sphaeroides* in negative ion mode (A and B) and in positive ion mode (C and D). The highlighted peaks in panel A are those of CL at *m/z* 1456, 1430, and 1428, which are barely discernible in panel B, which shows the CL(−) sample. (A) CL(+) membranes in negative ion mode. (B) CL(−) membranes in negative ion mode. (C) CL(+) membranes in positive ion mode. (D) CL(−) membranes in positive ion mode. Each was at a membrane protein concentration of 0.25 mg/mL. The identities of labeled ions in each spectrum were confirmed by MS/MS experiments. Ions labeled with asterisks were identified as 2,5-DHB matrix cluster adducts. The peaks at *m/z* 1495.9, 1497.9, 1533.8, and 1535.8 were determined by MS/MS and MS^n not to be CL or CL derivatives.

procedures.[50] These facts, along with the good agreement with the radioactive labeling analysis (Table 1) and quantitative ESI measurements described in Figures 2 and 4 of the companion paper (DOI 10.1021/bi1017039), lend strength to the quantitative significance of the observation of the approximately 5% relative abundance of CL ions in CL(−) membranes compared to CL(+) membranes. The 5% level is calculated relative to the ion abundances of PE 18:1/18:1 at *m/z* 742.5 and SQDG 18:1/18:1 and SQDG 18:0/18:1 at *m/z* 845.5 and 847.5, respectively, the most abundant ions within the displayed *m/z* range (Figure 5A,B). In contrast, the abundance of the PG 18:1/18:1 (*m/z* 773.5) and the SQDG 16:0/18:1 and SQDG 16:0/18:0 (*m/z* 819.5 and 821.5, respectively) lipid species showed an apparent increase in the CL(−) mutant membrane. (It should be noted that the *m/z* 1495.9 and 1497.9 ions seen in negative ion mode were determined not to be related to cardiolipin by MS/MS and MS^3 analysis.)

The positive ion mode MALDI MS spectra of the membranes of the CL(+) and CL(−) strains are shown in panels C and D of Figure 5, respectively. In addition to the most abundant PC lipid ions [PC 18:1/18:1 (*m/z* 786, 808, and 824) and PC 18:1/19:1 (*m/z* 800 and 838)], PE lipids [mainly PE 18:1/18:1 (*m/z* 744 and 766)] and ornithine lipids [OL 3-OH 20:1/19:1 (*m/z* 719)] were also observed in positive ion mode. The recently discovered glutamine lipids (QL)[53] were also identified by ESI analysis of the membrane lipid extract [Supporting Information of the companion paper (DOI 10.1021/bi1017039)]; QL has a relatively lower ionization efficiency in MALDI and overlaps with the ion at *m/z* 719 of OL. Comparison of Figure 5C with Figure 5D suggests that PC, PE, and OL are not significantly affected by the *cls* mutation, either in molecular structural diversity or in relative quantity.

Purification and Crystallization of CcO from the Wild Type and the *cls* Mutant. The *R. sphaeroides* strain containing the *cls* deletion and a plasmid containing CcO designed for crystallization (169CL3) displayed high expression yields. The UV−vis spectral characteristics of the CcO purified from this CL(−) strain, in reduced and oxidized forms, were essentially identical in the peak positions of hemes *a* and a_3 to those of the CcO obtained from the CL(+) strain purified in the same manner (Figure 6).

The CcO purified from CL(+) and CL(−) strains contained the normal four subunits (I, II, III, and IV) as revealed by SDS−PAGE analyses [see the companion paper (DOI 10.1021/bi1017039)]. Using CcO purified from CL(+) and CL(−) strains, CcO crystals were obtained with four subunits and with two subunits (subunits I and II only) for both strains, under the same crystallization conditions and yielding the same form (space group $P2_12_12_1$ for the two-subunit crystal and *R*3 for the four-subunit crystal). The resolution obtained for the four-subunit CcO crystals from the CL(−) mutant (3.2 Å) was similar

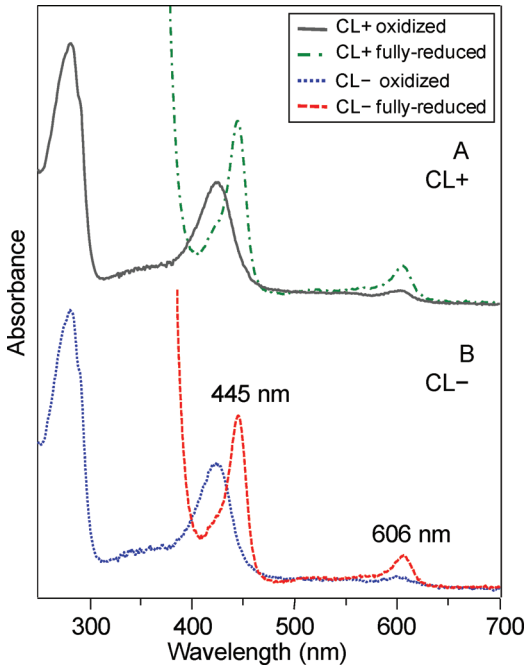

Figure 6. Oxidized and reduced spectra of purified C*c*O samples used to produce protein crystals, purified from (A) CL(+) (169WT) and (B) CL(−) (169CL3) strains grown aerobically at 30 °C. The reduced peaks at 445 and 606 nm, which are characteristic of the native heme *a* and a_3 spectra, are seen to be at the same wavelengths in both C*c*O forms. These peaks have contributions from both hemes at both wavelengths. The spectra were recorded using the same C*c*O protein concentrations.

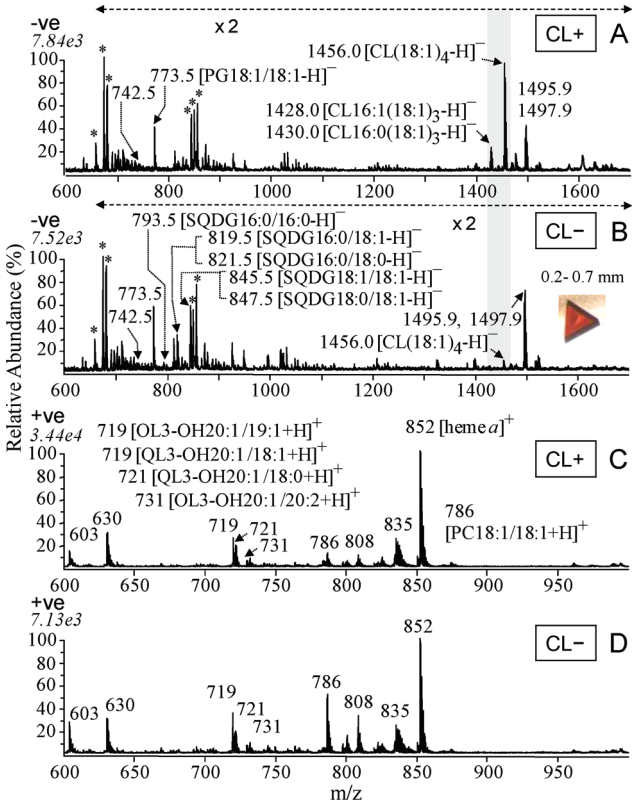

Figure 7. MALDI-MS spectra of the four-subunit C*c*O protein crystals from CL(+) (169WT) and CL(−) (169CL3) strains of *R. sphaeroides* in negative ion mode (A and B) and positive ion mode (C and D), showing a marked difference in CL content by relative peak height at *m*/*z* 1456 (highlighted). (A) C*c*O from CL(+) in negative ion mode. (B) C*c*O from CL(−) in negative ion mode. (C) C*c*O from CL(+) in positive ion mode. (D) C*c*O from CL(−) in positive ion mode. Ions labeled with asterisks were identified as 2,5-DHB matrix cluster adducts. The identities of labeled ions in each spectrum were confirmed by MS/MS experiments. The inset in panel B shows a photo of a typical four-subunit C*c*O crystal used in this analysis.

to that of four-subunit crystals from the CL(+) strain (3.3 Å), while the resolution for the two-subunit crystals from the CL(−) mutant (3.3 Å) was slightly less than that from the CL(+) strain (2.9 Å) based on many repeats with the CL(+) and CL(−) forms, grown, purified, and crystallized in parallel over several years (Table S2 of the Supporting Information). Thus, the strongly decreased levels of CL observed in the membrane lipid profile did not prevent the crystallization of four-subunit or two-subunit C*c*O. The four-subunit C*c*O crystals generated were examined by MALDI MS and MS/MS analysis.

MALDI MS and MS/MS Analysis of the Lipids in the Redissolved Four-Subunit C*c*O Crystals. Figure 7 shows the MALDI MS spectra obtained by direct analysis of the redissolved crystals, in negative ion mode (Figure 7A,B) and in positive ion mode (Figure 7C,D).

The data show that C*c*O crystals from the CL(+) strain retain readily detectable and multiple species of CL and SQDG, as well as PG 18:1/18:1 and OL 3-OH 20:1/19:1 in negative ion mode (Figure 7A) and PC18:1/18:1 and PE18:1/18:1 in positive ion mode, as confirmed by MS/MS analysis (Figures 8 and 9). These detailed structures of the lipids in the crystals have not been previously reported. Both cardiolipin and SQDG contained multiple fatty acid chain compositions. In addition to the most abundant $CL(18:1)_4$ (*m*/*z* 1456), minor species $CL(16:1)_1(18:1)_3$ (*m*/*z* 1428) and $CL(16:0)_1(18:1)_3$ (*m*/*z* 1430) were also found, in ratios similar to those found in the membrane, indicating no apparent selection for CL on the part of C*c*O during purification and crystallization. SQDG in the crystals also included a variety of fatty acid chain compositions (Figure 9B,C), all at comparable relative abundances. The relative levels of various fatty acids appear to be representative of the membrane background (compare Figure 7 and Figure 5), suggesting that C*c*O also has little selectivity for fatty acid chain variations in SQDG.

In the C*c*O crystals from the CL(−) mutant, MS clearly reveals significantly decreased levels of CL (Figure 7B) equivalent to those in the CL(−) membrane (Figure 5B), as well as an apparently higher abundance of SQDG species (*m*/*z* 793, 819, 821, 845, and 847) compared to the CL(+) crystal (Figure 7A). MS/MS further demonstrates that the level of $CL(18:1)_4$ (*m*/*z* 1456) in the CL-deficient mutant crystal is ~10% of that seen in the wild type, as indicated by comparison of the absolute abundances of the *m*/*z* 699 fragment ion (the 18:1/18:1 phosphatidyldioleoylglyceride ion)[50,54] in the MS/MS spectra of the *m*/*z* 1455.9 precursor ions from CL(−) and CL(+) crystals (Figure 8A,B). These results are again consistent with the membrane CL levels and with radioactive labeling (Table 1), suggesting no strong selectivity of C*c*O for CL in a CL(−) membrane environment. The PG lipid species (*m*/*z* 773.5) exhibit increases in abundance to some extent, while PE, PC, and OL lipids are observed in MS positive ion mode to be at relative levels similar to those in the crystals of the CL(+) strain (Figure 7C,D).

It is noteworthy that the major molecular species of cardiolipin in the isolated cell membranes and the C*c*O crystals of *R. sphaeroides* has four 18:1 fatty acyl chains, $CL(18:1)_4$ (*m*/*z* 1456), and the three

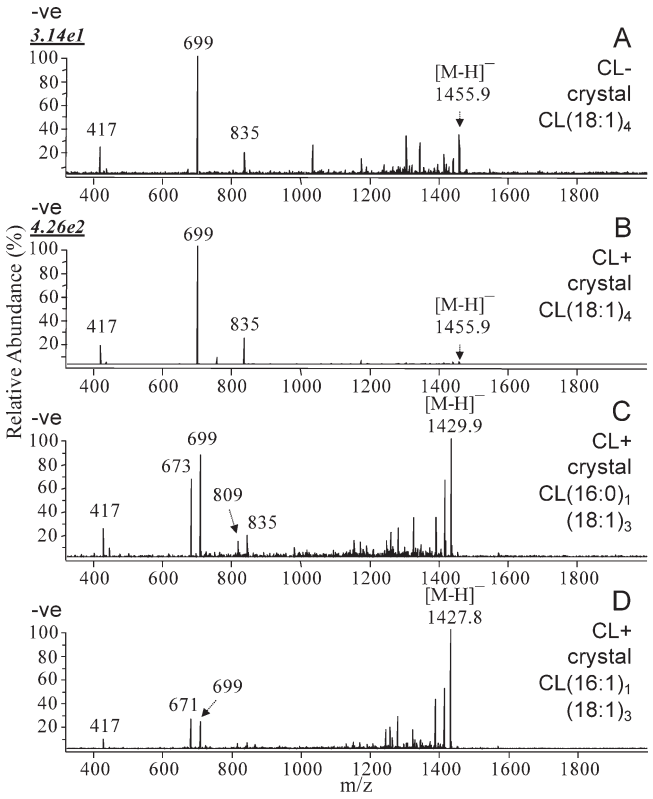

Figure 8. Identification of the cardiolipin molecular species in the four-subunit C*c*O crystals from CL(+) (169WT) and CL(−) (169CL3) *R. sphaeroides* using CID MS/MS in negative ion mode on a MALDI linear ion trap mass spectrometer, showing the marked depletion of $CL(18:1)_4$ in CL(−) crystals compared to CL(+) crystals (A and B) as demonstrated by comparison of the absolute ion abundance of *m/z* 699 (top left of panels A and B), the predominant product ion generated by $CL(18:1)_4$ in MS/MS, corresponding to the phosphatidyldioleoylglyceride moiety. The figure identifies multiple CL species in CL(+) C*c*O crystals (B−D), but no $CL(18:2)_4$ at *m/z* 1448 is seen (see also Figure 7A).

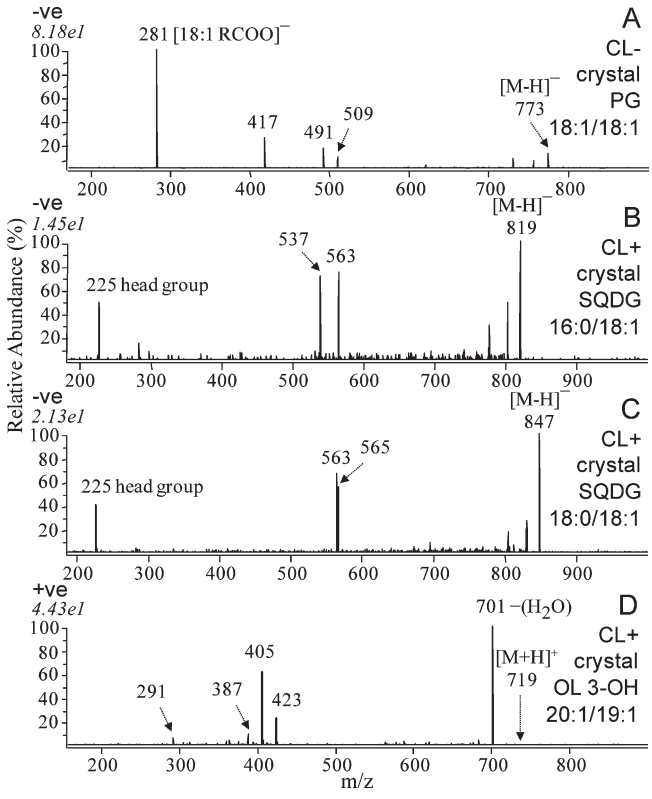

Figure 9. MS/MS spectra showing the characteristic fragmentation patterns of the precursor ions of the major lipids, providing the identifications of these lipids in the C*c*O crystals from CL(+) (169WT) and CL(−) (169CL3) *R. sphaeroides* using CID MS/MS in positive and negative ion modes on a MALDI linear ion trap mass spectrometer. Representative lipids in the crystals include (A) PG 18:1/18:1 at *m/z* 773 (−ve), (B) SQDG 16:0/18:1 at *m/z* 819 (−ve), (C) SQDG 18:0/18:1 at *m/z* 847 (−ve), and (D) OL 3-OH 20:1/19:1 at *m/z* 719 (+ve). In panels B and C, the fragment ion at *m/z* 225 is determined by MS^3 to represent the sulfoquinovosyl headgroup of SQDG, and the peaks in the middle of the spectra are generated by the neutral loss of either of the two fatty acid chains.

minor species of cardiolipin are $CL(16:1)_1(18:1)_3$, $CL(16:0)_1(18:1)_3$, and $CL(18:0)_1(18:1)_3$. However, $CL(18:2)_4$ [tetralinoleoyl cardiolipin (*m/z* 1448)], the predominant cardiolipin species found in mammalian mitochondria,[29,55] was not observed in any of the samples of *R. sphaeroides* examined in this study.

DISCUSSION

Residual CL in the Cardiolipin-Deficient Mutant. The *cls*-encoded enzyme catalyzes the synthesis of CL from two PG molecules.[56] Although lipid analysis showed a significant reduction in the level of CL in the mutant membranes, a small amount of CL (<10% of the amount of the wild type) still persisted in both the membrane and the C*c*O crystals of the mutant, as confirmed by saturation radioactive labeling, MALDI MS, MALDI MS/MS, and ESI with internal standards [companion paper (DOI 10.1021/bi1017039)]. At this reduced CL level, no appreciable effects on protein expression, protein spectroscopic properties, activity, assembly, and crystallization were observed.

The source of this residual CL in the mutant still needs to be determined. In the *E. coli cls* knockout mutant, overexpression of the *pss* gene led to an increase in the CL level,[49] suggesting that phosphatidylserine synthase has CL synthase activity. In a similar experiment, it has been observed that the expression of the *pss* gene (GenBank entry YP_353797) from *R. sphaeroides* in the *E. coli* SD9 strain resulted in the synthesis of CL (up to 1%), which exhibited dependence on the level of expression of the gene.[43] Thus, as observed for *E. coli*, phosphatidylserine synthase may be the source of the residual CL in the CL3 mutant of *R. sphaeroides*.[43]

Difference between Molecular Components of CL in *R. sphaeroides* and Mammalian Cells. Mass spectrometry analysis revealed that the CL molecular species in the membrane, the purified C*c*O enzymes, and the C*c*O protein crystals is mainly $CL(18:1)_4$, while much less abundant $CL(16:1)_1(18:1)_3$, $CL(16:0)_1(18:1)_3$, and $CL(18:0)_1(18:1)_3$ were also present. In contrast to the mammalian mitochondria, in which $CL(18:2)_4$ is the predominant and functionally essential species,[29,55,57] *R. sphaeroides* contained no $CL(18:2)_4$ that could be detected by MS. Cardiolipin in mammalian mitochondria has been proposed to be a part of the signaling system in apoptosis, involving the peroxidizability of the 18:2 unsaturated fatty acyl chains and not the 18:1 acyl chain components.[29,55,58] The predominant CL species in healthy mammalian mitochondria is

$CL(18:2)_4$, and a relative decrease in the level of the 18:2 cardiolipin component has been correlated with diseased mitochondria.[29,55] $CL(18:2)_4$ is also found to activate mammalian C*c*O more efficiently than other lipids.[59] Notably, $CL(18:2)_4$ is not synthesized directly in mammalian cells but is formed through a modification by acyltransferases of the initial cardiolipin species,[58] a process that is absent from the bacterial systems.[58,60] Yeasts also predominantly produce cardiolipin containing 16:1 and 18:1 fatty acyl chains but not 18:2.[61,62] The observed difference in cardiolipin types may account for fundamental differences in the functional roles that cardiolipin plays in the bacterial, yeast, and mammalian systems.

CL and Growth of *R. sphaeroides*. The CL3 mutant exhibited some decreased level of growth under respiratory conditions, suggesting that a normal level of CL is important for robust respiratory growth. A similar effect of CL deficiency on respiratory growth has been observed in a *Saccharomyces cerevisiae crd1*Δ mutant, in which the loss of CL affects the stability of the respiratory chain complexes.[25,26,63] The photosynthetic growth of the CL3 mutant was not affected, probably because other lipids such as PG substituted for CL. It has been shown that the level of PG is preferentially increased in purple bacteria during photosynthetic growth.[64] It is possible that the level of CL needed for photosynthetic growth is not as high as that needed for respiratory growth, and therefore, the low level of CL retained by the CL3 mutant could be sufficient under photosynthetic conditions.

Alternatively, CL may be required only during stress situations. Osmotic stress during growth has been shown to increase the level of CL synthesis in *R. sphaeroides*.[65] Variable, but often lower, levels of C*c*O production are observed from CL3 cultures, a response that may be due to the added stress of subculturing, dilution, and growth at high oxygen levels and high pH (approaching stationary phase). Determining a specific role of CL during respiratory growth in *R. sphaeroides* will require further studies.

CL in the Function and Assembly of C*c*O of *R. sphaeroides*. Low levels of CL did not appreciably affect the assembly or activity of the purified enzyme (Table 2). The C*c*O produced the same type of four-subunit crystals that diffracted to the same level as crystals from the CL(+) strains (Table S2 of the Supporting Information). It was critical to determine whether, despite the low CL levels, C*c*O was able to preferentially sequester enough CL for its needs. However, the MS and MS/MS analyses reproducibly demonstrated that the purified enzyme and the crystals did not concentrate CL above that found in the membranes. It is reasonable to conclude that CL is not essential for the structure, function, or crystallization of *Rhodobacter* C*c*O, consistent with several previous studies using bacterial and yeast systems.[30−32] This is in contrast to numerous biochemical and biophysical studies that suggest a requirement for CL in mammalian systems.[7,29,58,66]

A CL requirement for maintaining supercomplexes between C*c*O and other membrane proteins of the respiratory chain, and not for the stability or activity of C*c*O per se, could still be the case in *R. sphaeroides*, because evidence of such complexes is also found in other bacterial systems.[67] Experiments in yeast suggest that complexes III (bc_1) and IV (C*c*O) do not form the normal level of supercomplexes in the mitochondria of CL-deficient mutants, and CL-deficient yeast cultures also grew more slowly and to a lower final density than wild-type yeast cultures.[25] Similarly, the CL3 mutant grew more slowly under respiratory conditions used in this study (Figure 3), but no direct evidence to support a role in supercomplex formation is available.

The mass spectrometric data on C*c*O suggest that other lipids may functionally substitute for CL in *R. sphaeroides*. A relative increase in the levels of SQDG and PG was observed in crystals from the CL(−) mutant strain (Figure 7B). The increase in the level of PG in the CL(−) mutant was also observed in the membrane samples by radioisotope labeling (Table 1). Earlier studies comparing the yeast *cls* mutant (CL-deficient) and *pgs* mutant (PG- and CL-deficient) suggested that CL is not essential for the functions of C*c*O or mitochondria in yeast[30−32] but can be functionally replaced by PG.[30] The lack of difference in SQDG levels observed in membrane preparations, when analyzed either by thin-layer chromatography or by mass spectrometry, suggests that the altered levels seen in the crystals by MS may reflect some selectivity of C*c*O, rather than a general metabolic response at the cellular level. Specifically bound SQDG molecules have been previously resolved in the crystals of cyanobacterial photosystem II[68,69] but not yet in *R. sphaeroides* C*c*O. The apparent increased abundance of SQDG in the C*c*O crystals suggests a possible compensatory role for SQDG during CL deficiency, because both are anionic lipids and the level of SQDG was found to increase in *R. sphaeroides* membranes under phosphate-limiting growth conditions.[39] Studies in *Rhodobacter capsulatus*, which has neither CL nor an aa_3-type oxidase, have suggested a similar function for ornithine lipid.[70] This type of lipid is present in the *R. sphaeroides* membranes[53] but is not appreciably altered in CL(−) membranes, as seen by thin-layer chromatography and mass spectrometry.

In a previous study, Qin et al.[2] obtained high-resolution (2.0 Å) two-subunit C*c*O crystals that contain a potential CL binding site, based on homology with the bovine enzyme, even though the headgroup is not resolved. In our study, the two-subunit crystal form was produced from both CL(+) and CL(−) strains, but in neither case was the resolution sufficiently high for visualization of the lipids, likely due to the background strain, 2.4.1, not containing the necessary deletion of subunit IV that has been found to be key to giving the highest-resolution crystals.[2]

Lipid Mutants of *R. sphaeroides* as Tools for the Study of Membrane Proteins in Vivo. One of the motivations for studying the production, properties, and crystallization of C*c*O in the CL-deficient mutant of *R. sphaeroides* was to test the hypotheses that (1) CL is a necessary component of the fully functional enzyme in *R. sphaeroides* and (2) the specific lipid composition of a membrane protein sample is an important factor in producing high-quality crystals. The basis for the first hypothesis was a wealth of biochemical evidence supporting a role for CL in C*c*O function in mammalian systems.[7,12,20,66] The basis for the second hypothesis was the observation of specifically bound and conserved lipids in high-resolution crystal structures of membrane proteins. A further motivation for these studies was to establish *R. sphaeroides* as a tool for the overproduction of membrane proteins from many sources for structural studies[71] by providing versions of *R. sphaeroides* with different and controlled lipid compositions.

The results herein, especially the MS lipid analysis of the C*c*O crystals, argue against both starting hypotheses and suggest that C*c*O in *R. sphaeroides* does not have a strict requirement for CL per se. The results demonstrate that it is possible to overproduce C*c*O in a CL-deficient mutant and that the purified enzyme is fully active by available criteria and gives well-resolved crystals, despite a very low CL content. The ability to directly analyze the

lipid content of the crystals provides unique insight into the effects of low levels of CL, showing the presence of other bacterial lipids, including SQDG and ornithine lipid, apparently substituting for CL in the crystal. To determine the extent to which the roles of CL can be fully played by other lipid species in *R. sphaeroides*, we developed a method for further perturbing the lipid profile and producing a more complete CL deficiency, using a combined metabolic and genetic approach [see the companion paper (DOI 10.1021/bi1017039)].

■ ASSOCIATED CONTENT

Supporting Information. *R. sphaeroides* strains and C*c*O plasmids used in this work (Table S1) and X-ray screening results of C*c*O crystals obtained from C*c*O expressed in the *R. sphaeroides* wild-type CL(+) and CL(−) mutant at different crystal growth temperatures (Table S2). This material is available free of charge via the Internet at http://pubs.acs.org.

■ AUTHOR INFORMATION

Corresponding Author

*Department of Biochemistry and Molecular Biology, Michigan State University, East Lansing, MI 48824. Phone: (517) 353-3512. Fax: (517) 353-9334. E-mail: fergus20@msu.edu.

Author Contributions

X.Z. and B.T. contributed equally to this work.

Funding Sources

The work was supported by National Institutes of Health Grant R01 GM26916 (S.F.-M.) and the Michigan State University Center of Excellence for the Structural Analysis of Membrane Proteins (C.B., G.E.R., and S.F.-M.).

■ ACKNOWLEDGMENT

We thank Dr. Koichiro Awai for help with the design of the *cls* gene disruption strategy and Dr. Ling Qin for assistance in crystallizing C*c*O. We are grateful to Dr. Kouji Matsumato (Saitama University, Saitama-shi, Japan) for providing the *E. coli* CL-deficient mutant. Crystal screening was conducted at Argonne National Laboratories, APS synchrotron, LS CAT beamline.

■ ABBREVIATIONS

C*c*O, cytochrome *c* oxidase; *cls*, cardiolipin synthase gene; CL, cardiolipin; PG, phosphatidylglycerol; PE, phosphatidylethanolamine; PC, phosphatidylcholine; OL, ornithine lipid; QL, glutamine lipid; SQDG, sulfoquinovosyldiacylglyceride; CL(+), cardiolipin-proficient strain; CL(−), cardiolipin-deficient strain; MALDI, matrix-assisted laser desorption ionization; nESI, nanoelectrospray ionization; MS, mass spectrometry; MS/MS, tandem mass spectrometry; MS^n, multistage tandem mass spectrometry; 2,5-DHB, 2,5-hydroxybenzoic acid; SDS−PAGE, sodium dodecyl sulfate−polyacrylamide gel electrophoresis; TLC, thin-layer chromatography; PCR, polymerase chain reaction; WT, wild type.

■ REFERENCES

(1) Cherezov, V., Rosenbaum, D. M., Hanson, M. A., Rasmussen, S. G., Thian, F. S., Kobilka, T. S., Choi, H. J., Kuhn, P., Weis, W. I., Kobilka, B. K., and Stevens, R. C. (2007)High-resolution crystal structure of an engineered human β2-adrenergic G protein-coupled receptor. *Science 318*, 1258–1265.

(2) Qin, L., Hiser, C., Mulichak, A., Garavito, R. M., and Ferguson-Miller, S. (2006)Identification of conserved lipid/detergent-binding sites in a high-resolution structure of the membrane protein cytochrome c oxidase. *Proc. Natl. Acad. Sci. U.S.A. 103*, 16117–16122.

(3) Nussberger, S., Doerr, K., Wang, D. N., and Kuhlbrandt, W. (1993)Lipid-protein interactions in crystals of plant light-harvesting complex. *J. Mol. Biol. 234*, 347–356.

(4) Bogdanov, M., Sun, J., Kaback, H. R., and Dowhan, W. (1996)A phospholipid acts as a chaperone in assembly of a membrane transport protein. *J. Biol. Chem. 271*, 11615–11618.

(5) Bogdanov, M., and Dowhan, W. (1998)Phospholipid-assisted protein folding: Phosphatidylethanolamine is required at a late step of the conformational maturation of the polytopic membrane protein lactose permease. *EMBO J. 17*, 5255–5264.

(6) Bogdanov, M., Umeda, M., and Dowhan, W. (1999)Phospholipid-assisted refolding of an integral membrane protein. Minimum structural features for phosphatidylethanolamine to act as a molecular chaperone. *J. Biol. Chem. 274*, 12339–12345.

(7) Sedlák, E., and Robinson, N. C. (1999)Phospholipase A_2 digestion of cardiolipin bound to bovine cytochrome *c* oxidase alters both activity and quaternary structure. *Biochemistry 38*, 14966–14972.

(8) Valiyaveetil, F. I., Zhou, Y., and MacKinnon, R. (2002)Lipids in the structure, folding, and function of the KcsA K^+ channel. *Biochemistry 41*, 10771–10777.

(9) Lange, C., Nett, J. H., Trumpower, B. L., and Hunte, C. (2001) Specific roles of protein-phospholipid interactions in the yeast cytochrome bc1 complex structure. *EMBO J. 20*, 6591–6600.

(10) Awasthi, Y. C., Chuang, T. F., Keenan, T. W., and Crane, F. L. (1971)Tightly bound cardiolipin in cytochrome oxidase. *Biochim. Biophys. Acta 226*, 42–52.

(11) Gomez, B., Jr., and Robinson, N. C. (1999)Phospholipase digestion of bound cardiolipin reversibly inactivates bovine cytochrome bc1. *Biochemistry 38*, 9031–9038.

(12) Robinson, N. C. (1982)Specificity and binding affinity of phospholipids to the high affinity cardiolipin sites of beef heart cytochrome *c* oxidase. *Biochemistry 21*, 184–188.

(13) Schagger, H., Hagen, T., Roth, B., Brandt, U., Link, T. A., and von Jagow, G. (1990)Phospholipid specificity of bovine heart bc_1 complex. *Eur. J. Biochem. 190*, 123–130.

(14) Zhang, H., Kurisu, G., Smith, J. L., and Cramer, W. A. (2003)A defined protein-detergent-lipid complex for crystallization of integral membrane proteins: The cytochrome b6f complex of oxygenic photosynthesis. *Proc. Natl. Acad. Sci. U.S.A. 100*, 5160–5163.

(15) Garavito, R. M., and Ferguson-Miller, S. (2001)Detergents as tools in membrane biochemistry. *J. Biol. Chem. 276*, 32403–32406.

(16) Guan, L., Smirnova, I. N., Verner, G., Nagamori, S., and Kaback, H. R. (2006)Manipulating phospholipids for crystallization of a membrane transport protein. *Proc. Natl. Acad. Sci. U.S.A. 103*, 1723–1726.

(17) Hosler, J. P., Ferguson-Miller, S., and Mills, D. A. (2006)Energy transduction: Proton transfer through the respiratory complexes. *Annu. Rev. Biochem. 75*, 165–187.

(18) Mills, D. A., and Ferguson-Miller, S. (2003)Understanding the mechanism of proton movement linked to oxygen reduction in cytochrome c oxidase: Lessons from other proteins. *FEBS Lett. 545*, 47–51.

(19) Marsh, D., and Horvath, L. I. (1998)Structure, dynamics and composition of the lipid-protein interface. Perspectives from spin-labelling. *Biochim. Biophys. Acta 1376*, 267–296.

(20) Powell, G. L., Knowles, P. F., and Marsh, D. (1987)Spin-label studies on the specificity of interaction of cardiolipin with beef heart cytochrome oxidase. *Biochemistry 26*, 8138–8145.

(21) Distler, A. M., Allison, J., Hiser, C., Qin, L., Hilmi, Y., and Ferguson-Miller, S. M. (2004)Mass spectrometric detection of protein, lipid and heme components of cytochrome *c* oxidase from *R. sphaeroides* and the stabilization of non-covalent complexes from the enzyme. *Eur. Mass Spectrom. 10*, 295–308.

(22) Svensson-Ek, M., Abramson, J., Larsson, G., Tornroth, S., Brzezinski, P., and Iwata, S. (2002)The X-ray crystal structures of wild-type and EQ(I-286) mutant cytochrome *c* oxidases from *Rhodobacter sphaeroides*. *J. Mol. Biol. 321*, 329–339.

(23) Fyfe, P. K., Isaacs, N. W., Cogdell, R. J., and Jones, M. R. (2004) Disruption of a specific molecular interaction with a bound lipid affects the thermal stability of the purple bacterial reaction centre. *Biochim. Biophys. Acta 1608*, 11–22.

(24) Palsdottir, H., and Hunte, C. (2004)Lipids in membrane protein structures. *Biochim. Biophys. Acta 1666*, 2–18.

(25) Zhang, M., Mileykovskaya, E., and Dowhan, W. (2002)Gluing the respiratory chain together. Cardiolipin is required for supercomplex formation in the inner mitochondrial membrane. *J. Biol. Chem. 277*, 43553–43556.

(26) Pfeiffer, K., Gohil, V., Stuart Rosemary, A., Hunte, C., Brandt, U., Greenberg Miriam, L., and Schagger, H. (2003)Cardiolipin stabilizes respiratory chain supercomplexes. *J. Biol. Chem. 278*, 52873–52880.

(27) Sorice, M., Manganelli, V., Matarrese, P., Tinari, A., Misasi, R., Malorni, W., and Garofalo, T. (2009)Cardiolipin-enriched raft-like microdomains are essential activating platforms for apoptotic signals on mitochondria. *FEBS Lett. 583*, 2447–2450.

(28) Tyurin, V. A., Tyurina, Y. Y., Ritov, V. B., Lysytsya, A., Amoscato, A. A., Kochanek, P. M., Hamilton, R., Dekosky, S. T., Greenberger, J. S., Bayir, H., and Kagan, V. E. (2010)Oxidative lipidomics of apoptosis: Quantitative assessment of phospholipid hydroperoxides in cells and tissues. *Methods Mol. Biol. 610*, 353–374.

(29) Sparagna, G. C., Chicco, A. J., Murphy, R. C., Bristow, M. R., Johnson, C. A., Rees, M. L., Maxey, M. L., McCune, S. A., and Moore, R. L. (2007)Loss of cardiac tetralinoleoyl cardiolipin in human and experimental heart failure. *J. Lipid Res. 48*, 1559–1570.

(30) Chang, S.-C., Heacock, P. N., Mileykovskaya, E., Voelker, D. R., and Dowhan, W. (1998)Isolation and characterization of the gene (CLS1) encoding cardiolipin synthase in *Saccharomyces cerevisiae*. *J. Biol. Chem. 273*, 14933–14941.

(31) Tuller, G., Hrastnik, C., Achleitner, G., Schiefthaler, U., Klein, F., and Daum, G. (1998)YDL142c encodes cardiolipin synthase (Cls1p) and is non-essential for aerobic growth of *Saccharomyces cerevisiae*. *FEBS Lett. 421*, 15–18.

(32) Jiang, F., Rizavi, H. S., and Greenberg, M. L. (1997)Cardiolipin is not essential for the growth of *Saccharomyces cerevisiae* on fermentable or non-fermentable carbon sources. *Mol. Microbiol. 26*, 481–491.

(33) Sistrom, W. R. (1960)A requirement for sodium in the growth of *Rhodopseudomonas spheroides*. *J. Gen. Microbiol. 22*, 778–785.

(34) Sistrom, W. R. (1962)The kinetics of the synthesis of photopigments in *Rhodopseudomonas spheroides*. *J. Gen. Microbiol. 28*, 607–616.

(35) Benning, C., and Somerville, C. R. (1992)Isolation and genetic complementation of a sulfolipid-deficient mutant of *Rhodobacter sphaeroides*. *J. Bacteriol. 174*, 2352–2360.

(36) Zhen, Y., Qian, J., Follmann, K., Hayward, T., Nilsson, T., Dahn, M., Hilmi, Y., Hamer, A. G., Hosler, J. P., and Ferguson-Miller, S. (1998)Overexpression and purification of cytochrome c oxidase from *Rhodobacter sphaeroides*. *Protein Expression Purif. 13*, 326–336.

(37) van Niel, C. B. (1944)The Culture, General Physiology, Morphology, and Classification of the Non-Sulfur Purple and Brown Bacteria. *Bacteriol. Rev. 8*, 1–118.

(38) Yeliseev, A. A., and Kaplan, S. (2000)TspO of *Rhodobacter sphaeroides*. A structural and functional model for the mammalian peripheral benzodiazepine receptor. *J. Biol. Chem. 275*, 5657–5667.

(39) Benning, C., Beatty, J. T., Prince, R. C., and Somerville, C. R. (1993)The sulfolipid sulfoquinovosyldiacylglycerol is not required for photosynthetic electron transport in *Rhodobacter sphaeroides* but enhances growth under phosphate limitation. *Proc. Natl. Acad. Sci. U.S.A. 90*, 1561–1565.

(40) Simon, R., Priefer, U., and Puehler, A. (1983)Vector plasmids for in vivo and in vitro manipulations of Gram-negative bacteria. *Mol. Genet. Bact.—Plant Interact., [Symp.]*, 98–106.

(41) Weissenmayer, B., Geiger, O., and Benning, C. (2000)Disruption of a gene essential for sulfoquinovosyldiacylglycerol biosynthesis in *Sinorhizobium meliloti* has no detectable effect on root nodule symbiosis. *Mol. Plant—Microbe Interact. 13*, 666–672.

(42) Arondel, V., Benning, C., and Somerville, C. R. (1993)Isolation and functional expression in *Escherichia coli* of a gene encoding phosphatidylethanolamine methyltransferase (EC 2.1.1.17) from *Rhodobacter sphaeroides*. *J. Biol. Chem. 268*, 16002–16008.

(43) Tamot, B. (2006) Construction and characterization of a cardiolipin-deficient mutant in *Rhodobacter sphaeroides*. M.S. Thesis, Department of Biochemistry and Molecular Biology, Michigan State University, East Lansing, MI.

(44) Hosler, J. P., Fetter, J., Tecklenburg, M. M. J., Espe, M., Lerma, C., and Ferguson-Miller, S. (1992)Cytochrome aa3 of *Rhodobacter sphaeroides* as a model for mitochondrial cytochrome c-oxidase. Purification, kinetics, proton pumping, and spectral analysis. *J. Biol. Chem. 267*, 24264–24272.

(45) Smith, P. K., Krohn, R. I., Hermanson, G. T., Mallia, A. K., Gartner, F. H., Provenzano, M. D., Fujimoto, E. K., Goeke, N. M., Olson, B. J., and Klenk, D. C. (1985)Measurement of protein using bicinchoninic acid. *Anal. Biochem. 150*, 76–85.

(46) Qin, L., Mills, D. A., Buhrow, L., Hiser, C., and Ferguson-Miller, S. (2008)A conserved steroid binding site in cytochrome *c* oxidase. *Biochemistry 47*, 9931–9933.

(47) Altschul, S. F., Madden, T. L., Schaffer, A. A., Zhang, J., Zhang, Z., Miller, W., and Lipman, D. J. (1997)Gapped BLAST and PSI-BLAST: A new generation of protein database search programs. *Nucleic Acids Res. 25*, 3389–3402.

(48) Shibuya, I., Miyazaki, C., and Ohta, A. (1985)Alteration of phospholipid composition by combined defects in phosphatidylserine and cardiolipin synthases and physiological consequences in *Escherichia coli*. *J. Bacteriol. 161*, 1086–1092.

(49) Nishijima, S., Asami, Y., Uetake, N., Yamagoe, S., Ohta, A., and Shibuya, I. (1988)Disruption of the *Escherichia coli cls* gene responsible for cardiolipin synthesis. *J. Bacteriol. 170*, 775–780.

(50) Zhang, X. (2009) Investigating the functional roles of lipids in membrane protein cytochrome *c* oxidase from *Rhodobacter sphaeroides* using mass spectrometry and lipid profile modification. Ph.D. Thesis, Department of Chemistry and Department of Biochemistry and Molecular Biology, Michigan State University, East Lansing, MI.

(51) Klug, R. M., and Benning, C. (2001)Two enzymes of diacylglyceryl-O-4′-(N,N,N,-trimethyl)-homoserine biosynthesis are encoded by btaA and btaB in the purple bacterium *Rhodobacter sphaeroides*. *Proc. Natl. Acad. Sci. U.S.A. 98*, 5910–5915.

(52) Busch, K. L. (2003)Chemical noise in mass spectrometry. Part III. More mass spectrometry/mass spectrometry. *Spectroscopy (Duluth, MN, U.S.) 18*, 52–55.

(53) Zhang, X., Ferguson-Miller, S. M., and Reid, G. E. (2009) Characterization of ornithine and glutamine lipids extracted from cell membranes of *Rhodobacter sphaeroides*. *J. Am. Soc. Mass Spectrom. 20*, 198–212.

(54) Hsu, F.-F., Turk, J., Rhoades Elizabeth, R., Russell David, G., Shi, Y., and Groisman Eduardo, A. (2005)Structural characterization of cardiolipin by tandem quadrupole and multiple-stage quadrupole ion-trap mass spectrometry with electrospray ionization. *J. Am. Soc. Mass Spectrom. 16*, 491–504.

(55) Sparagna, G. C., Johnson, C. A., McCune, S. A., Moore, R. L., and Murphy, R. C. (2005)Quantitation of cardiolipin molecular species in spontaneously hypertensive heart failure rats using electrospray ionization mass spectrometry. *J. Lipid Res. 46*, 1196–1204.

(56) Hirschberg, C. B., and Kennedy, E. P. (1972)Mechanism of the enzymatic synthesis of cardiolipin in *Escherichia coli*. *Proc. Natl. Acad. Sci. U.S.A. 69*, 648–651.

(57) Han, X., Yang, J., Yang, K., Zhao, Z., Abendschein, D. R., and Gross, R. W. (2007)Alterations in myocardial cardiolipin content and composition occur at the very earliest stages of diabetes: A shotgun lipidomics study. *Biochemistry 46*, 6417–6428.

(58) Chicco, A. J., and Sparagna, G. C. (2007)Role of cardiolipin alterations in mitochondrial dysfunction and disease. *Am. J. Physiol. 292*, C33–C44.

(59) Yamaoka-Koseki, S., Urade, R., and Kito, M. (1991)Cardiolipins from rats fed different dietary lipids affect bovine heart cytochrome *c* oxidase activity. *J. Nutr. 121*, 956–958.

(60) Lopez-Lara, I. M., Sohlenkamp, C., and Geiger, O. (2003) Membrane lipids in plant-associated bacteria: Their biosyntheses and possible functions. *Mol. Plant-Microbe Interact. 16*, 567–579.

(61) Schlame, M., and Greenberg, M. L. (1997)Cardiolipin synthase from yeast. *Biochim. Biophys. Acta 1348*, 201–206.

(62) Gaspar, M. L., Aregullin, M. A., Jesch, S. A., Nunez, L. R., Villa-Garcia, M., and Henry, S. A. (2007)The emergence of yeast lipidomics. *Biochim. Biophys. Acta 1771*, 241–254.

(63) Zhong, Q., Gohil, V. M., Ma, L., and Greenberg, M. L. (2004) Absence of cardiolipin results in temperature sensitivity, respiratory defects, and mitochondrial DNA instability independent of pet56. *J. Biol. Chem. 279*, 32294–32300.

(64) Russell, N. J., and Harwood, J. L. (1979)Changes in the acyl lipid composition of photosynthetic bacteria grown under photosynthetic and non-photosynthetic conditions. *Biochem. J. 181*, 339–345.

(65) Catucci, L., Depalo, N., Lattanzio, V. M. T., Agostiano, A., and Corcelli, A. (2004)Neosynthesis of cardiolipin in *Rhodobacter sphaeroides* under osmotic stress. *Biochemistry 43*, 15066–15072.

(66) Robinson, N. C., Zborowski, J., and Talbert, L. H. (1990) Cardiolipin-depleted bovine heart cytochrome *c* oxidase: binding stoichiometry and affinity for cardiolipin derivatives. *Biochemistry 29*, 8962–8969.

(67) Berry, E. A., and Trumpower, B. L. (1985)Isolation of ubiquinol oxidase from *Paracoccus denitrificans* and resolution into cytochrome bc1 and cytochrome c-aa3 complexes. *J. Biol. Chem. 260*, 2458–2467.

(68) Loll, B., Kern, J., Saenger, W., Zouni, A., and Biesiadka, J. (2005)Towards complete cofactor arrangement in the 3.0 Å resolution structure of photosystem II. *Nature 438*, 1040–1044.

(69) Jones, M. R. (2007)Lipids in photosynthetic reaction centres: Structural roles and functional holes. *Prog. Lipid Res. 46*, 56–87.

(70) Aygun-Sunar, S., Mandaci, S., Koch, H.-G., Murray, I. V. J., Goldfine, H., and Daldal, F. (2006)Ornithine lipid is required for optimal steady-state amounts of *c*-type cytochromes in *Rhodobacter capsulatus*. *Mol. Microbiol. 61*, 418–435.

(71) Laible, P. D., Scott, H. N., Henry, L., and Hanson, D. K. (2004) Towards higher-throughput membrane protein production for structural genomics initiatives. *J. Struct. Funct. Genomics 5*, 167–172.